Transactions in GIS, 2004, 8(1): 83–111

Research Article

The Effect of DEM Raster Resolution on First Order, Second Order and Compound Terrain Derivatives

Stefan Kienzle
Department of Geography
University of Lethbridge

Abstract
It is well known that the grid cell size of a raster digital elevation model has significant effects on derived terrain variables such as slope, aspect, plan and profile curvature or the wetness index. In this paper the quality of DEMs derived from the interpolation of photogrammetrically derived elevation points in Alberta, Canada, is tested. DEMs with grid cell sizes ranging from 100 to 5 m were interpolated from 100 m regularly spaced elevation points and numerous surface-specific point elevations using the ANUDEM interpolation method. In order to identify the grid resolution that matches the information content of the source data, three approaches were applied: density analysis of point elevations, an analysis of cumulative frequency distributions using the Kolmogorov-Smirnov test and the root mean square slope measure. Results reveal that the optimum grid cell size is between 5 and 20 m, depending on terrain complexity and terrain derivative. Terrain variables based on 100 m regularly sampled elevation points are compared to an independent high-resolution DEM used as a benchmark. Subsequent correlation analysis reveals that only elevation and local slope have a strong positive relationship while all other terrain derivatives are not represented realistically when derived from a coarse DEM. Calculations of root mean square errors and relative root mean square errors further quantify the quality of terrain derivatives.

1 Introduction

The proliferation of digital elevation sources and terrain analysis tools enables researchers and operators in environmental science, agriculture, hydrology, biology and engineering to compute terrain-dependent variables and indices easier than ever before. Today, all

Address for correspondence: Stefan Kienzle, Department of Geography, University of Lethbridge, 4401 University Drive, Lethbridge, Alberta, T1K 3M4, Canada. E-mail: stefan.kienzle@uleth.ca

desktop GISs, as well as stand-alone processing tools such as Terrain Analysis Programs for the Environmental Sciences (grid version: TAPES-G, described in, e.g. Moore et al. 1991, Gallant and Wilson 1996), USGS's Spatial Terrain Analysis Resource Toolset (START, see Blaszcynski 1997), SOLARFLUX (Hetrick et al. 1993a, b) or TOPOVIEW (Helios Environmental Modeling Institute [HEMI], 1999), offer a range of terrain analysis options. They extend from slope and aspect analyses using a variety of algorithms (e.g. Evans 1980, Horn 1981, Zevenbergen and Thorne 1987) to the estimation of more sophisticated terrain attributes such as the drainage network (e.g. Jenson and Domingue 1988, Tarboton et al. 1991, Garbrecht and Martz 1997), the topographic wetness index (Beven and Kirkby 1979) or radiation fluxes (e.g. Hetrick et al. 1993a, Moore et al. 1993, Quinn and Beven 1993). By using one or several terrain variables and indices, a catchment area can be characterized in terms of geomorphology (e.g. Jenson and Domingue 1988, Moore et al. 1993), stream network patterns (e.g. Tarboton et al. 1991, Band 1993) or landform classification (Blaszcynski 1997, Macmillan et al. 2000). Subsequently, ecosystem modelling, such as modelling the distribution of energy, water, sediments, nutrients (e.g. Mitasova et al. 1996, Kienzle et al. 1997, Klaghofer et al. 1993) and pollutants (e.g. Kern and Stednick 1993), depends on realistic terrain representation.

The three dominant formats for DEMs are square-grid rasters, triangular irregular networks (TINs) and contour-based networks (Moore et al. 1991). The raster or grid structure consists of square or rectangular grid cells arranged in rows and columns and represents the mean elevation for each grid cell. Raster-based DEMs are very widely used because of their simplicity and computational efficiency (Martz and Garbrecht 1992). They are continuous elevation fields and are predominantly interpolated from point and/or line data with known or estimated elevation values. There are many mathematical functions available to fit a smooth surface through the sampled elevation points, such as inverse distance weighting, splining, local and global polynomial trend surfaces, kriging or specialized algorithms such as ANUDEM (Hutchinson 1989, 1991). Typically, each algorithm has a range of parameters that needs to be set, and results may differ significantly from one another (Burrough and McDonnell 1998, Garbrecht and Martz 2000). The root mean square (RMS) error, a measure of the accuracy of the interpolated surface, can be large (Blöschl and Grayson 2001). Some algorithms, such as inverse distance weighting, are poorly suited to interpolate a DEM from irregularly sampled elevation points due to the creation of unrealistically shaped terrain features, often referred to as "bull's eyes". Algorithms which offer the best results include the regular spline with tension (Hofierka et al. 2002) and ANUDEM, based on a thin-plate splining technique with additional features resulting in realistic terrain representation. Local errors in the interpolation of DEMs can be very large.

In addition to problems with generating a DEM per se, the quality of a DEM depends on the quality and density of sampled elevation points and the raster resolution, expressed in grid cell size. Most higher resolution digital elevation data available today have been derived from photogrammetry, using stereo aerial photographs with a range of scales. The Shuttle Radar Topography Mission (SRTM) is currently in its final project phase and will provide elevation data with a 30 m horizontal resolution, covering the entire planet up to a latitude of 60° north and south. In recent years, high resolution LIDAR (Light Detection And Ranging) data are becoming increasingly popular and available, but the comparatively high cost limits its use to relatively small study areas. For the province of Alberta, Canada, elevation data with the highest spatial resolution

are provided by AltaLIS, the agent for Spatial Data Warehouse, which is a not-for-profit organization maintaining and promoting Alberta's digital mapping. DEMs are available for the so-called "white area", which is the surveyed area of Alberta. These elevation data sets are available in 100 m regular grids with many additional surface-specific point elevations to define the framework of the terrain, including spot heights and points along ridges, streams and saddles. A data set covers one 1:20,000 map sheet area. DEMs and DTMs (digital terrain models, containing terrain variables such as slope, aspect or curvature rather than elevation values) based on this data set are referred to as DEM_{100} or DTM_{100}. Point elevation data are in Digital Mapping Data Format (DMDF). Alberta Agriculture, Food and Rural Development (AAFRD) have developed DEMs from this data set for internal use with grid resolutions of 100 m and 25 m (Parkinson 2002, pers. comm.).

It is well known that most terrain attributes derived from a DEM change with a variation in the underlying grid cell size. Figure 1 illustrates the impact that the interpolated grid cell size has on terrain representation. Elevations were interpolated to grid cell sizes of 100, 50, 25 and 5 m, using the same input data and interpolation algorithm (ANUDEM; Hutchinson 1989, 1991). Then a profile line was draped over the four elevation models, and elevation values were extracted at an interval associated with the respective DEM resolution. It is evident from Figure 1 that terrain features such as slope,

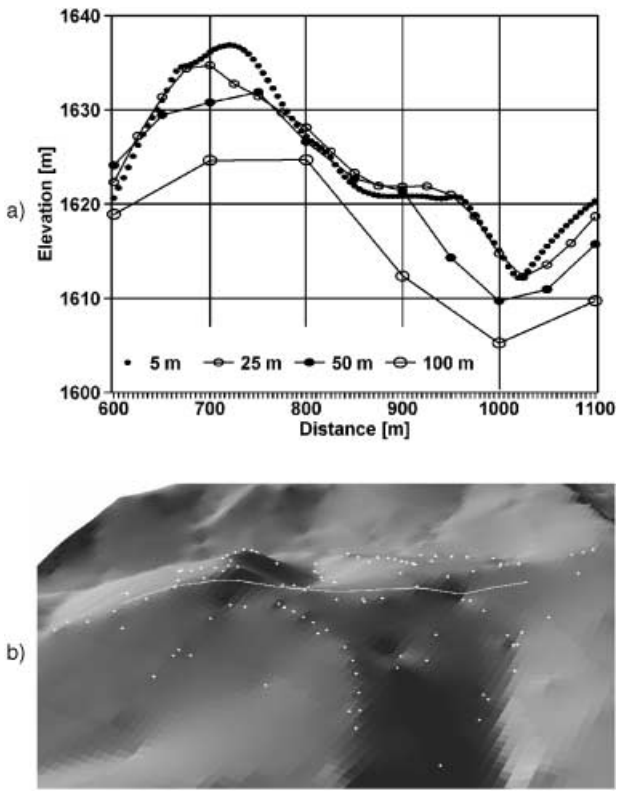

Figure 1 (a) Effect of interpolated DEM resolution on terrain profiles; (b) visualization of profile line and surrounding elevation points draped over a DEM with 5 m grid cell size, 2 times vertical exaggeration

Table 1 Geomorphological parameters estimated from DEMs with varying grid cell size in the Henley catchment, KwaZulu-Natal, South Africa

Variable	Grid cell size	Mean	Max
Slope [%]	250 m	8.8	33
	100 m	13.4	85.5
	50 m	13.9	143.2
Soil loss potential [t ha^{-1} $year^{-1}$]	250 m	21.4	164
	100 m	31.3	303
	50 m	35.4	603

aspect or upslope area will depend on DEM resolution. Previous studies have shown that the DEM grid cell size significantly affects derived terrain parameters (Kienzle 1994, Zhang and Montgomery 1994, Elsheikh and Guercio 1997). Kienzle (1994) has used terrain variables to distinguish between terrain units and estimate soil erosion potential for catchments in South Africa. He determined that in the 179 km^2 Henley Dam catchment in the Midlands of KwaZulu-Natal, South Africa, both slope and soil erosion estimations increase with a decrease in interpolated grid cell size (Table 1). Saulnier et al. (1997) investigated the analytical compensation between DEM grid resolution and hydrological terrain derivatives and found, for example, that the topographic index, which combines the local slope and the associated upslope area, increases with grid cell size. This means that catchments are modelled to be wetter using a coarse grid cell size and drier using a finer grid resolution. Other investigators, such as Zhang and Montgomery (1994), used photogrammetrically sampled elevation data and compared grid cell sizes ranging from 2 to 90 m for two small catchments in Oregon (Mettman Ridge catchment) and California, USA (Tennessee Valley catchment). They derived a mean slope of 65% and 34% for the 2 m grid and 41% and 29% for the 90 m grid and found that the grid size significantly affects the cumulative frequency distributions of the specific catchment area, topographic index and, consequently, the hydrological simulations.

One can summarize that the ability to carry out realistic terrain analyses is limited primarily by the quality of the DEM applied in terms of:

- the accuracy and distribution of the elevation points used to interpolate the DEM
- the interpolation algorithm used to generate a continuous DEM, and
- the chosen grid cell size

and will affect subsequent modelling of surface processes, such as erosion, deposition, slope stability, hydrological or water quality processes.

A grid cell size is often selected not with a specific subsequent terrain analysis in mind, but to overlay a DEM with other raster data such as satellite imagery, where the grid cell size is predetermined. While this is an important consideration, one should be aware of the consequences that the grid cell size has on terrain analyses. For example, there may be merit in choosing a fraction of the given grid resolution such as 12.5 or 6.25 m grid cell sizes for overlay with 25 m resolution LANDSAT imagery. It is important to know the exact grid cell size and projection of other raster data before one begins the creation of a DEM.

In this paper, the author systematically assesses how grid cell size affects terrain derivatives using elevation points available in Alberta, Canada, by applying the same interpolation algorithm and two sets of photogrammetrically derived elevation points at two different scales. Terrain derivatives of the first and second order are investigated as well as the wetness index representing compound terrain derivatives. This analysis also allows one to statistically define the grid resolution that corresponds to the content of the source data. Issues associated with the quality of sampled elevation points or various DEM interpolation techniques are not addressed.

2 Study Area

In order to represent areas typical for the Rocky Mountain foothills and Great Plains regions of western North America (Figure 2), three areas were chosen with steep (Study Area 1), moderately sloped (Study Area 2) and flat (Study Area 3) relief (Figure 3). Mountainous areas with very steep slopes are not investigated. Study Area 4 lies within the city boundaries of Lethbridge and is used to compare the DEM derived from the provincial elevation database to one with a higher resolution. Table 2 lists some key terrain parameters to characterize the different study areas.

Study Areas 1 to 3 are square areas, containing a small watershed of about 7 km^2, and are 3.6 by 3.6 km in size. This size was chosen because it is a multiple of all grid cell sizes that are to be investigated, thus eliminating possible errors in calculating terrain derivatives along the edges. Study Area 4 is 1.5 by 1.5 km in size and lies to the

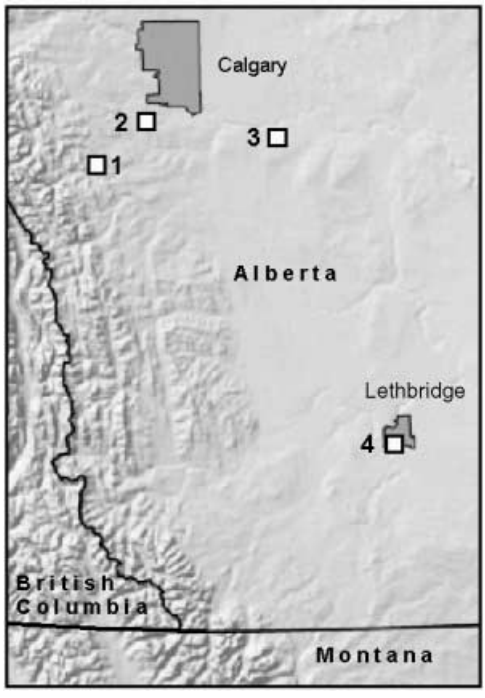

Figure 2 Location of four study areas

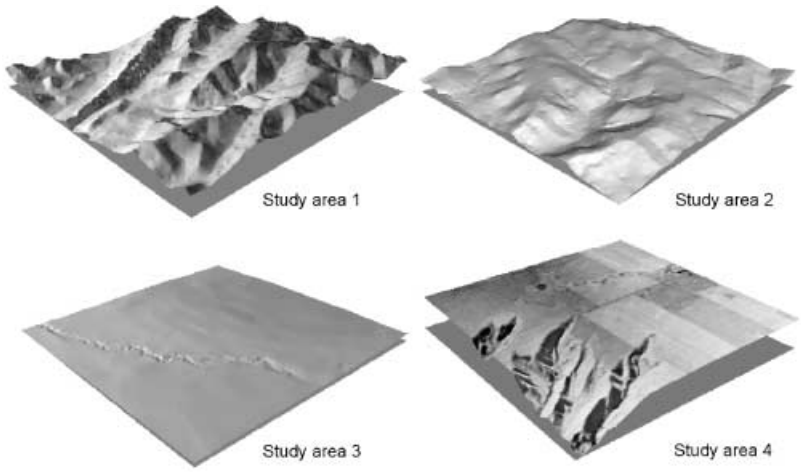

Figure 3 Terrain visualization of four study areas

Table 2 Key terrain characteristics of the four study areas. Slope values are based on a 10 m DEM using Horn's (1981) method

Study Area	Scale of Aerial Photo	Size [km^2]	Density of sampled elevation points [points km^{-2}]	Mean slope [%]	Max Slope [%]	Elevation range [m]
1	1:60,000	15.21	484	24.1	78.4	326
2	1:60,000	15.21	251	12.3	55.9	235
3	1:60,000	15.21	178	1.1	18.1	66
4	1:60,000	2.25	345	3.9	34.7	107
4	1:10,000	2.25	11,162	4.1	33.8	105

west of the Oldman River within the city limits of Lethbridge. The area is not urbanized and includes very flat areas as well as steep slopes along the 60 m deep river valley.

Study Areas 1, 2 and 3 are used to determine significant differences in terrain derivatives from a variety of grid cell sizes under terrain conditions ranging from moderately steep to very flat. Study Area 4 is used to compare DEMs derived from two independent sources in order to reveal the quality of terrain attributes derived from the DEM_{100}, which is available for most of Alberta.

3 Analysis

3.1 Terrain Derivatives

Instead of analyzing elevation data directly, terrain derivatives are analyzed to reveal statistically significant differences. Slope and aspect (slope direction) are the first derivatives of the mathematically continuous surface that constitutes a raster DEM. Both Horn's and Zevenbergen and Thorne's algorithms are widely used, although numerous

Table 3 Terrain derivatives tested

Order of Derivative	Terrain attribute
First order derivatives	Slope (Horn) Slope (Zevenbergen and Thorne) Aspect (Horn) Aspect (Zevenbergen and Thorne)
Second order derivatives	Profile curvature Plan curvature
Combined derivatives	Curvature Wetness index

other slope and aspect estimators exist (Burrough and McDonnell 1998). Horn's (1981) third-order finite difference estimator is used by the SLOPE command in ArcView and ArcInfo (both products of Environmental Systems Research Institute Inc. 2000), whereas Zevenbergen and Thorne's (1987) second-order finite difference method is incorporated in ArcInfo's CURVATURE command. Jones (1998) investigated eight algorithms for calculating slope and aspect using both actual and manufactured DEMs. His research revealed that Zevenbergen and Thorne's method ranked best and Horn's method ranked second best. Florinsky (1998) prefers Evans's (1980) slope estimator, which was not included in Jones's (1998) comparative study.

The second order derivatives, the rates of change of slope in the down slope direction (profile curvature) and perpendicular to the down slope direction (plan curvature) are investigated because of their importance in geomorphological and hydrological analyses. Finally, terrain indices that combine two or more terrain attributes (compound derivatives) are analyzed because of their wide applications and expected sensitivity to grid resolution. The curvature, which is the product of plan and profile curvature, is important in modelling erosion and runoff processes. The second compound derivative chosen is the wetness index (also called the topographic index). It is extensively used in hydrology, agriculture, geomorphology and vegetation studies because it represents the spatial distribution of soil moisture, surface saturation, groundwater recharge and discharge areas, as well as potential runoff generation (variable source areas). Table 3 lists the terrain derivatives tested.

3.2 Comparison of Two Independent DEMs

In addition to identifying significant differences between important terrain derivatives for a variety of grid resolutions, the terrain derivatives are compared to an independently sampled, high resolution DEM. Major cities in Alberta have DEMs that are sampled photogrammetrically at 10 m regular intervals, referred to here as DEM_{10}. High resolution DEMs with grid cell sizes of 5 and 1 m are used to evaluate the errors of terrain derivatives based on the DEM_{100}. Correlation analysis is applied to reveal the strength of relationships between terrain derivatives based on the two independent data sources. Using the DEM_{10} as a benchmark, RMS and relative root mean square (RRMS)

errors are computed for elevation and terrain derivatives to indicate the quality of terrain derivatives based on DEM_{100}.

3.3 Preparation of Elevation Points

In order to generate the various DEMs, elevation points derived photogrammetrically from 1:60,000 scale aerial photos were acquired from AltaLIS. The data format had to be converted from the original Digital Map Data Format (DMDF) into an input format readable by ArcInfo. To retain the highest possible accuracy for the DEM, the original mm units were preserved in the transformation process and only after generation of the DEM were the data converted into a floating point grid with m units. Because of regular inconsistencies in coordinates (many X-coordinates were out by exactly 300 km) a conversion program identified all wrong coordinates and corrected them. In order to find three suitable smaller study areas, representing characteristic terrain in southern Alberta (excluding mountainous areas), an initial study area covering approximately 4,500 km^2 located south of Calgary was chosen. The spatial extent of each point data file is one 1:20,000 map sheet, which has an extent of 7.5′ latitude by 15.0′ longitude, with an over-edge of approximately 750 m.

After generating the point coverages, they were all merged into one point file for the study area. This resulted in having multiple points along the edges for similar locations, with up to four points along the corners of the map sheets. Elevations at the overlapping points were checked, and elevation differences were consistently less than 3 cm and therefore considered insignificant. All duplicate points were deleted. Figure 6 shows a typical distribution of elevation points over a sample terrain. About 1.8 million elevation points were initially analyzed. The elevation point density for the area ranges from 103 points per km^2 in the flatter eastern area to 850 points per km^2 in the more rugged western foothills region. Figure 4 shows the spatial distribution of sampling density for the study areas. It is evident from these figures that the sampling density increases with the complexity of the terrain, which is, of course, the result of the photogrammetric sampling technique

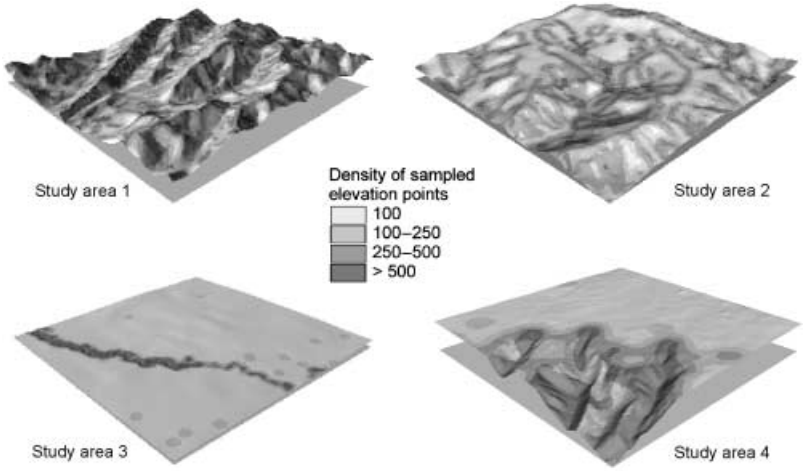

Figure 4 Density of sampled elevation points of four study areas (points per km^2)

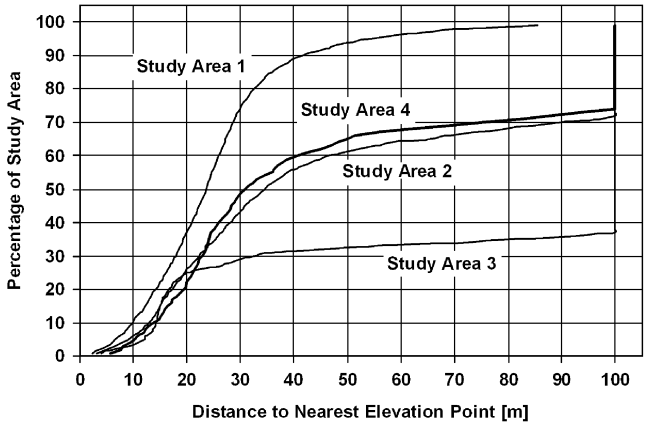

Figure 5 Cumulative frequency distributions of distances of nearest sampled elevation points of four study areas

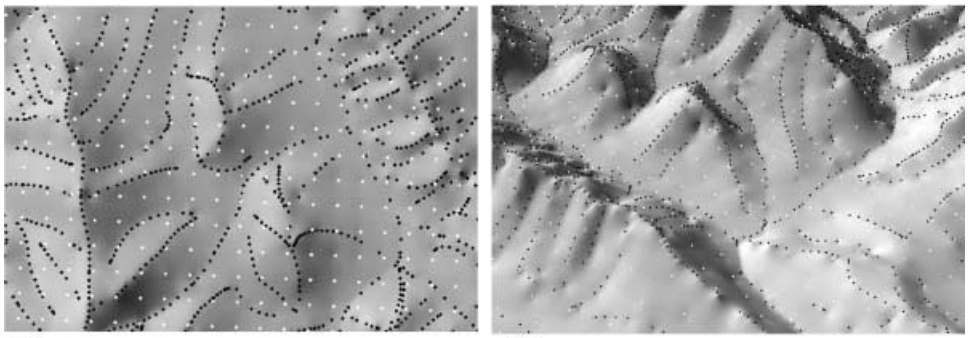

Figure 6 (a) 2D and (b) 3D view of a part of Study Area 1 with photogrammetrically derived elevation points draped over a hillshaded DEM with 5 m resolution that was generated from the points. The significance of spot heights and breakpoints becomes evident. White points are 100 m regularly sampled points; black points are breakpoints and spot heights

to represent the terrain properly at the scale of the aerial photographs. For a typical map sheet, there are about 27,000 elevation points sampled at regular 100 m intervals, and between 40,000 and 87,000 additional spot heights, break points and DEM structure lines, constituting between one third and more than two thirds of all sampled elevation points. From this initial DEM three study areas were chosen, which all contain a small watershed and differ both in slope and density of sampled elevation points (Table 2).

In order to determine the smallest grid cell size that can be used for the interpolated grids, the nearest distances between sampling points were calculated for the four study areas. The cumulative frequency distributions of the distances of the nearest sampled elevation points are shown in Figure 5. This graph shows that 50% of the point elevations in the study areas, with the exception of the very flat Study Area 3, have a nearest distance to each other of less than 24 m (Study Area 1), less than 30 m (Study Area 4) and less than

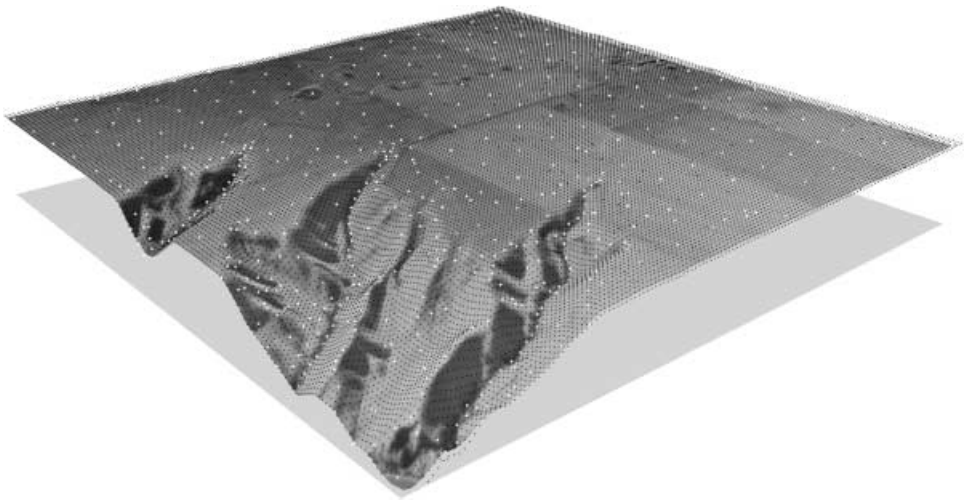

Figure 7 Distribution of photogrammetrically sampled elevation points over Study Area 4. The points as well as an aerial photograph are draped over a 1 m resolution DEM and displayed with a 2-times vertical exaggeration. White points are provided by AltaLIS and sampled at a 100 m regular interval with additionally sampled breakpoints and spot heights, while black points are provided by the City of Lethbridge and sampled at 10 m regular intervals, also with additional breakpoints and spot heights

35 m (Study Area 2). All study areas have sampled elevation points with a nearest distance of between 10 and 15 m for 10% of their area. Nearest distances can be as close as between 3 and 6 m. At locations where the sampling density is high (close distances between sampled elevation points) the terrain is typically complex (see Figures 4 and 6), which will locally affect slope, aspect, flow direction, erosion potential, radiation budgets, etc. Based on the local density, the smallest grid cell size that can be used from the DEM_{100} may be less than 10 m, and therefore grid cell sizes as low as 7.5 and 5 m were interpolated.

The fourth study area is situated in the City of Lethbridge. Elevation points for only one 1:20,000 map sheet were required, and AltaLIS data were imported in the same fashion as the other study areas. The high resolution city elevation points were imported into ArcInfo. The mean sampling density of the AltaLIS data set is 345 samples km^{-2}, while the city data set provided 11,162 samples km^{-2}. Figure 7 presents a comparison of both sampling densities for study area 4. This visual representation clearly indicates that some significant problems in the calculation of terrain derivatives from DEM_{100} can be expected.

3.4 Projection

It is important to project the point elevation file before the DEM generation in order to avoid later introduction of additional errors due to the resampling of the raster file during the projection process. The merged point file was projected from the original UTM, NAD83 projection into a projection specific to Alberta, the 3TM projection. This projection spans only 3 degrees, instead of UTM's 6 degrees, in an east-west direction and uses a scale factor of 0.9999 instead of UTM's 0.9996.

3.5 Interpolation of DEMs

It is important to note that the sensitivity of terrain derivatives to grid cell size is believed to be quite independent of the DEM interpolation algorithm used. While there are expected differences in derived terrain variables, generated from varying DEM interpolation methods, the overall patterns of the described variations of terrain variables with grid cell sizes and DEM sources are anticipated to be comparable. Future studies may quantify potential differences.

The TOPOGRID command in ArcInfo is an interpolation method specifically designed for the creation of hydrologically correct DEMs. TOPOGRID is based on the ANUDEM program (Australian National University Digital Elevation Model) developed by Hutchinson (1988, 1989). ANUDEM has been designed to produce accurate DEMs with realistic drainage properties from a comparatively small number of well-chosen elevation and stream line data sets. ANUDEM uses an iterative finite difference interpolation method. In this method, grid DEMs are calculated at successively finer resolutions, thereby combining the advantages of global interpolation methods with a local method. In addition, ANUDEM removes pits and uses stream information to ensure that the resulting DEMs are hydrologically correct. This makes this interpolation algorithm superior over other, purely mathematically based algorithms, because most terrain has been shaped geomorphologically by running water. In order to condition the interpolation process to produce a hydrologically correct terrain, a drainage enforcement algorithm removes erroneous depressions from the DEM (Hutchinson 1989). In addition, stream data take priority over point data. This required pre-processing of the stream coverage, which was available at the same scale as the point elevation data. The stream coverage had to be edited to avoid braided streams, parallel stream banks or lake polygons. The TOPOGRID command in ArcInfo, which incorporates the 1996 version of ANUDEM, requires that stream network data have all arcs pointing down slope. Consequently, an algorithm was applied to ensure that this condition was met. After proper preparation, the TOPOGRID command was executed to produce an initial DEM with a 25 m resolution.

Using this DEM, Study Areas 1, 2 and 3 were selected to represent three terrain types commonly found in southern Alberta. The size of the sub-sets was set to be 3,600 by 3,600 m, chosen to be a multiple of all grid cell sizes to be produced for the final analyses. During the subsequent execution of the TOPOGRID command the size of the sub-sets was increased in all directions by at least 20 times the chosen grid size to avoid potential edge problems of the resulting DEMs. The DEMs with resolutions of 100, 80, 75, 50, 30, 25, 20, 15, 12.5, 10, 7.5 and 5 m were then clipped to their original size of 3,600 by 3,600 m.

For Study Area 4 one section was made available by the City of Lethbridge. To avoid edge problems during the interpolation process, a central portion with the size 1,500 by 1,500 m was used as the final DEM.

3.6 Computation of Terrain Derivatives

The terrain derivatives were calculated for each DEM using the SLOPE (Horn's method), ASPECT (Horn's method) and CURVATURE (Zevenbergen and Thorne's method for slope, aspect, profile and plan curvatures, and compound curvature) commands in ArcInfo. The wetness index was calculated according to the equation:

$$w = \ln(A_s/\tan\beta) \tag{1}$$

where A_s is the specific catchment area (catchment area divided by the cell width in slope direction) and β is the local slope of the terrain in degrees (Beven and Kirkby 1979).

3.7 Statistical Analyses and Results

3.7.1 Comparison of terrain variables derived from different grid resolutions

For all terrain derivatives and all grid resolutions cumulative frequency distributions (CFDs) were computed. As an example, for the general patterns found, Figure 8 shows CFDs for five grid resolutions for slope, profile curvature and the wetness index for Study Area 1. The patterns presented in Figure 8 are the same for all four study areas. Generally, the larger the grid cell size the smaller the derived slope values (Figure 8a). The two different slope algorithms employed also reveal the same frequency distribution patterns, as is shown in Figures 10a and b. Differences in slope estimation are larger in terrain with high relief (Study Area 1) than in terrain with low relief (Study Area 3). Grid cell sizes over 25 m are not able to identify steep slopes successfully. This has a particular impact where slope stability or erosion is being estimated from relatively coarse DEMs. Calculated differences of slope generally become smaller with grid cell sizes under 25 m. Figure 9 presents a visualization of the DTM_{100} and shows the spatial distributions of slope values using DTM resolutions of 100, 50, 25, 10 and 5 m. It becomes evident that the 100 and 50 m DTMs, and to a lesser extent the 25 m DTM, result in a considerable underestimation of slope values, particularly along hillslopes.

The profile curvature is strongly underestimated using larger grid cell sizes (Figure 8b). A very similar pattern exists for plan curvature (Figures 10e and f). Again, the same patterns are found in all study areas. It becomes evident from Figures 8b, 10e and f that a characterization of an area in terms of concavity or convexity information fails to an increasing degree with larger DTM grid cell sizes. The impact of underestimating plan or profile curvatures is to underestimate dispersion and convergence areas, which are particularly important for erosion, sedimentation and hydrological analysis.

The wetness index, used as an example for compound terrain variables in Figure 8c, varies strongly with different grid resolutions. The general rule for all study areas is that with increasing grid cell size there is a more or less parallel shift towards higher wetness indices, with higher values indicating the potential for higher soil saturation. Therefore, when comparative studies between a number of watersheds are undertaken, the wetness would be overestimated with a coarser DEM. High relief terrain (Study Area 1) has lower mean wetness indices (6.3), representing drier soils, than terrain with moderate relief in Study Area 2 (7.2) and the flat Study Area 3 (9.4).

Based on the CFDs for Study Area 4, key percentiles were extracted and plotted against the grid resolution to reveal the sensitivity of the distribution parameters on grid cell size (Figure 10). In order to evaluate the distribution of terrain variables derived from DEM_{100}, the distribution values for terrain variables derived from a DEM_{10} are also displayed.

Figure 10 shows selected percentile values of the CFDs for Study Area 4 to reveal differences of terrain values as a function of both grid cell size and DTM source. In Figure 10, "10 m" signifies the DEM_{10} and "100 m" the DEM_{100}. There is a wealth of information that can be derived from this series of graphs. Slope grids with grid cell sizes of 15, 12.5, 10, 7.5 and 5 m have very similar distributions (Figures 10a and b) and show similar values even for the 99th percentile slope values, which represent the steepest one percent of the study area. Median slope values are also quite similar, although the larger grid cell sizes seem to slightly overestimate the median slope. This is due to the relatively

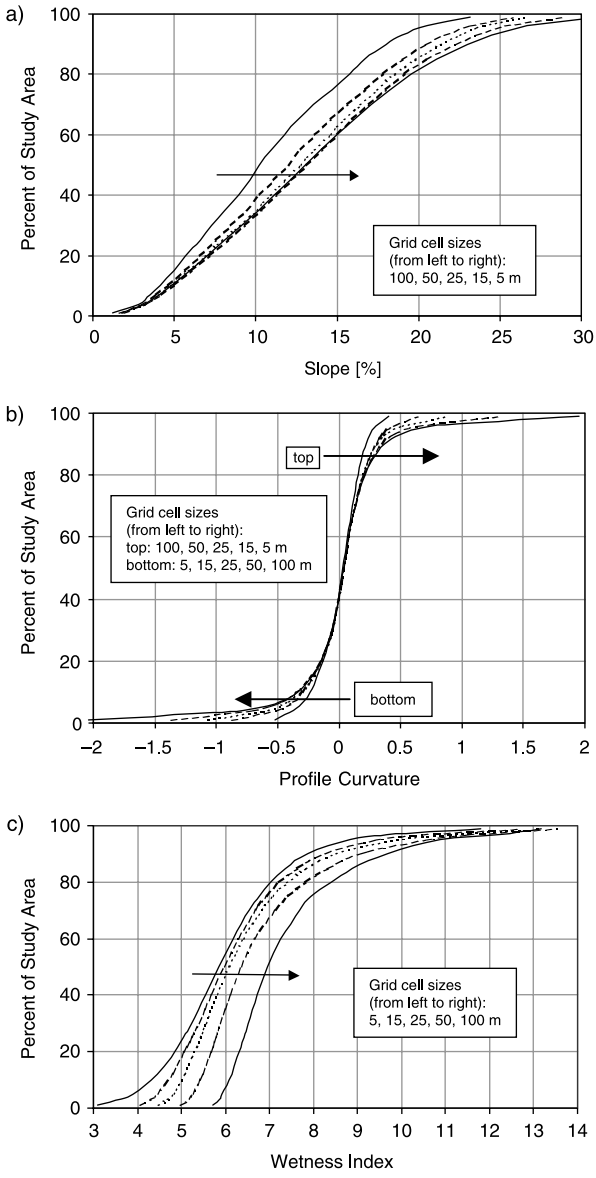

Figure 8 Cumulative frequency distributions for (a) slope, (b) profile curvature and (c) the wetness index for Study Area 1

greater number of grid cells associated with the valley slopes within the coarser DTMs. The slope distribution based on 5 m grid cell sizes of DTM_{100} and DTM_{10} compare favourably, indicating that an overall characterization of slope over a terrain similar to Study Area 4 can be represented by a 5 m DTM_{100}. Both the Horn and Zevenbergen and Thorne methods result in similar slope distribution values over the range of grid cell sizes investigated, with slope values derived using Zevenbergen and Thorne's method consistently being slightly higher (Figures 10a, b). Using the 10 m grid cell sizes based on

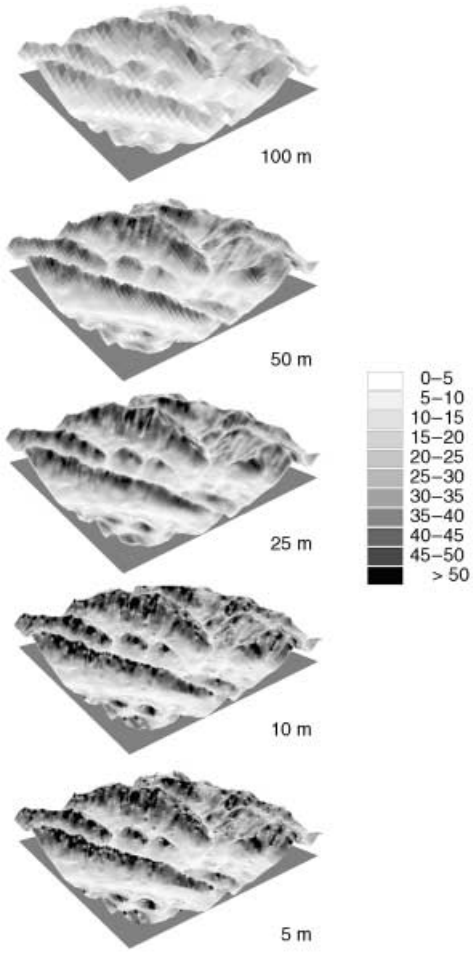

Figure 9 Comparison of slope distribution, derived from five different DEM resolutions

DEM_{10} as an example, median slope values are 2.11% (Horn) and 2.18% (Zevenbergen and Thorne), while the 95 percentile slope values are 35.98% and 36.53%, respectively.

Since a correct representation of aspect is crucial for the derivation of hydrological variables such as flow direction, flow accumulation, stream networks and catchment boundaries or environmental variables such as solar radiation or the wetness index, the potential misrepresentation of aspect values based on a DEM_{100} at any interpolated resolution may have significant consequences. In order to show the effects of grid resolution and DEM source, the differences in aspect angles were calculated, using the 5 m grid resolution based on DEM_{10} as a benchmark. An algorithm was developed to calculate the true angle differences between two grids in order to avoid challenges stemming from the fact that aspect angles of 359° and 1° are only 2° apart. Figures 10c and d show the key values of the frequency distribution of difference in aspect angle between grid cell sizes based on DEM_{100} and the 5 m grid cell size based on DEM_{10}. The results show that, virtually independent from the grid cell size chosen, the aspect angles based on

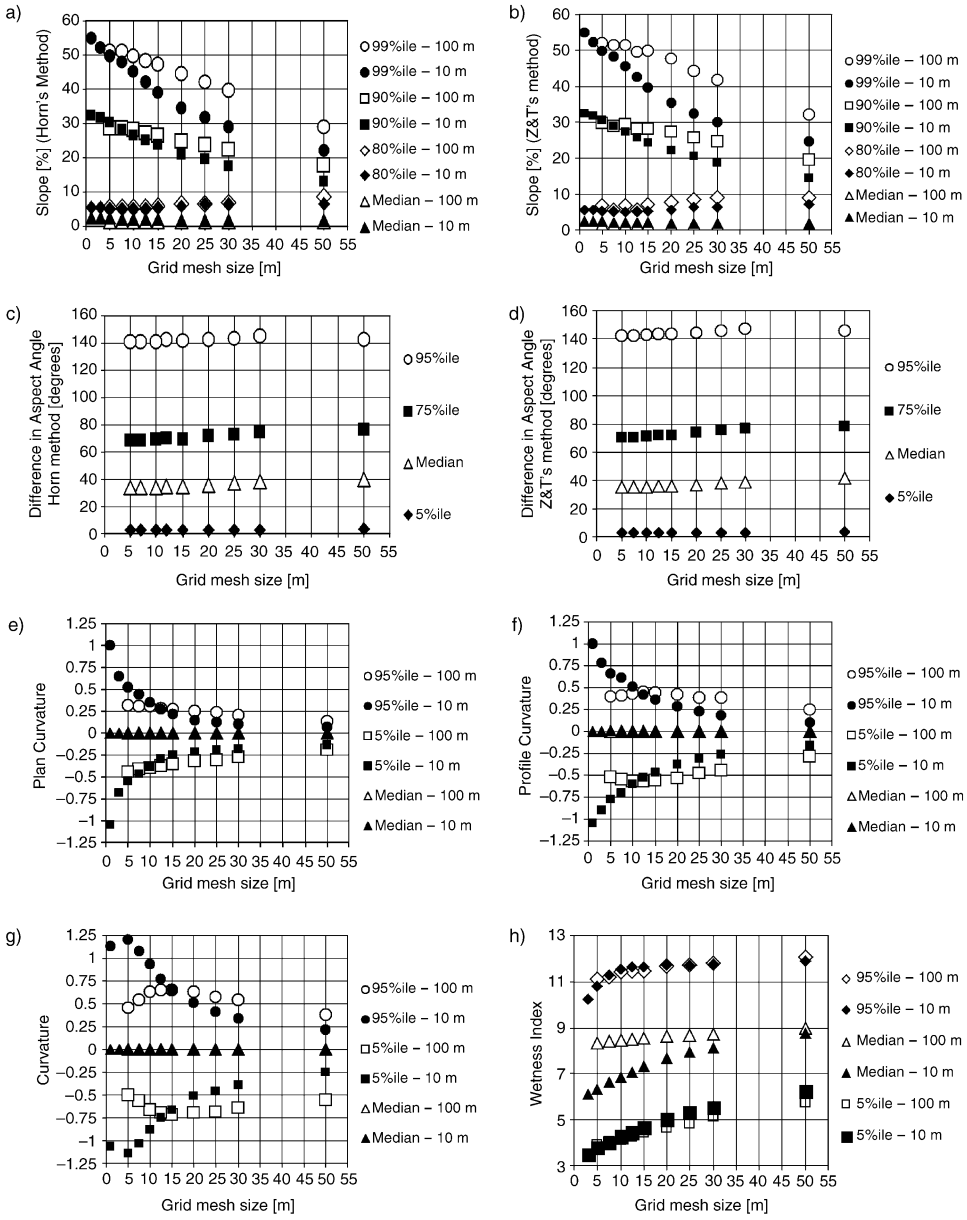

Figure 10 Key distribution values for terrain variables derived from a variety of DEM resolutions and generated from two independent sources for Study Area 4. In the legends, 100 m signifies DEM_{100}, and 10 m stand for DEM_{10}. Z & T is an abbreviation for Zevenbergen and Thorne (1987)

DEM_{100} are out by 35 to 40° for 50% of the study area, out by 70 to 80° for 25% of the study area (75th percentile) and may be as much out as 150° and, in less than 0.5% of cases, by a full 180°. No meaningful differences between the two algorithms used (Horn 1981, Zevenbergen and Thorne 1987) were observed.

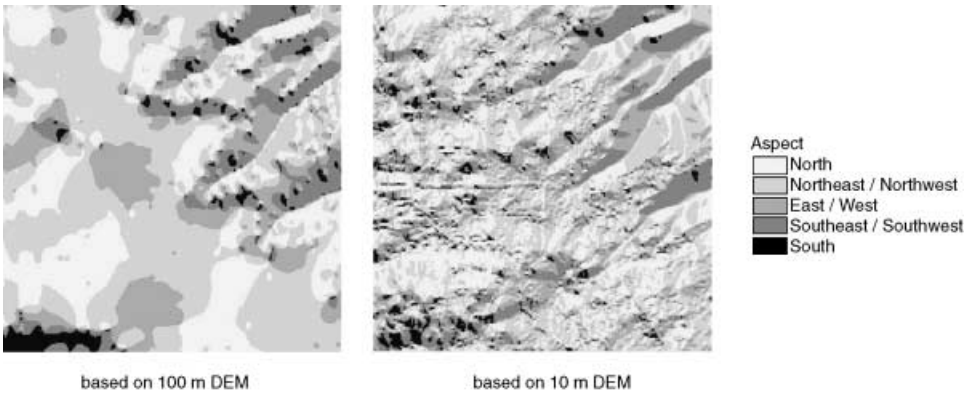

Figure 11 Comparison of aspect distribution based on two DEMs from different sources

Plan and profile curvature, as well as their product (curvature), show 95th percentile values that increase in range with decreasing grid cell size (Figures 10e, f, g), showing an increase in convexity or concavity with decreasing cell size. Median values are close to zero, which means that approximately the same level of concavity and convexity occurs within the study area. Plan and profile values are, however, reaching a limit in their range when they are based on the DEM_{100}. As was pointed out earlier, this may significantly affect calculations of overland flow and its divergence or convergence and subsequent erosion or deposition simulations. The limitations of the DEM_{100} for detailed hydrological or environmental terrain analyses become evident.

Figure 10h shows key percentiles for the distribution of the wetness index. The wetness index values become smaller (signifying drier soils) with a decrease in grid cell size. The overall distributions of wetness index values based on DEM_{10} or DEM_{100} are quite similar, but median index values based on DEM_{100} tend to be slightly larger than those based on DEM_{10}. The grid cell size is therefore critical when one compares wetness index values from different regions which may be based on different grid cell sizes and DEM sources.

The spatial distribution of aspect values at 5 m grid resolution from DEM_{100} and DEM_{10} are compared in Figure 11. The figure shows how aspect values derived from the DEM_{100} have significantly less local detail, particularly in the flat western and southern areas. While slope values can be represented quite well from DEM_{100}, aspect values may vary over small distances and are therefore much less realistic when derived from the coarse DEM_{100}. Figure 11 also shows some linear features in DTM_{10} in the SW quarter of the study area, which result from edge-matching problems stemming from the photogrammetric sampling process. Such linear features are a common problem with many DEMs and difficult to correct.

Figure 12 shows a visualization of Study Area 4 with the draped wetness index based on 5 m resolution derived from DTM_{100} and $DTM_{10.}$ It becomes evident that, particularly in flat terrain, the topographic position has a large impact on the wetness index, with low values (dry conditions) on small mounds and a concentration of potential water in shallow depressions, resulting in relatively high wetness index values there. Generally, within the flat part of Study Area 4, the wetness index values derived from DEM_{100} are considerably overestimated. This is largely due to problems in representing flow direction from DEM_{100}, which is imperative for the calculation of upslope areas, which, in turn, is used for the calculation of the wetness index. In steep terrain, the

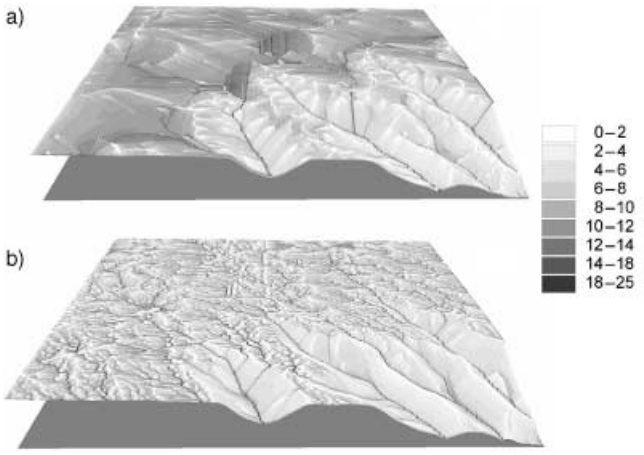

Figure 12 Comparison of the wetness index derived from 5 m grids generated from two different sources. (a) DEM_{100}, (b) DEM_{10}

wetness index compares more favourably between DEM_{100} and DEM_{10}. A comparison of flow direction and aspect values, calculated using different algorithms, shows very similar spatial distribution over Study Area 4.

While Figures 8 to 12 offer visual impressions of the sensitivity of terrain derivatives on grid resolution, they do not offer a quantification of the level of significant differences between terrain variables based on different grid cell sizes, nor can they quantify any spatial correlations between respective terrain variables based on DEM_{100} and the benchmark DEM_{10}.

3.7.2 Optimization of Grid Cell Size Using the Kolmogorov-Smirnov Test

The question arises: Which grid resolution corresponds to the information content of the source data? The first method used compares CFDs of terrain derivatives based on a number of different grid resolutions. In order to determine significant differences of terrain derivatives with decreasing grid cell size, each CFD was compared to the associated 5 m CFD by carrying out the two-sample Kolmogorov-Smirnov test. To be as unbiased as possible, only the grid cell sizes 80, 50, 30, 20, 12.5, 7.5 and 5 were used, because the ratio of two sequential cell sizes is consistently in a narrow range between 1.5 and 1.67. This test is the non-parametric equivalent to the two-sample t-test with unequal variances. It is typically applied when data sets to be compared are neither normally distributed nor meet the assumption of equal variances. The Kolmogorov-Smirnov test determines its test statistic by finding the point at which the two samples have the greatest difference between the cumulative proportions of the two samples. Consistently using 100 values representing all integer percentiles, the cumulative frequency distributions are considered different at the 95% confidence level when the maximum difference between the curves is greater than 0.1367. The differences must be greater than 0.1638 for the 99% confidence level. In cases where the difference between a 5 m grid and a 7.5 m grid was insignificant, and the difference between the 7.5 m grid and the 12.5 m grid was also insignificant, but the difference between the 5 m grid and the 12.5 m grid was significant, the 5 m grid would have been selected as the maximum grid cell to be used.

Table 4 Maximum grid cell sizes that are significantly different from the next larger grid cell size. Grid cell sizes tested are: 80, 50, 30, 20, 12.5, 7.5 and 5 m

Test Feature	Study Area (Sampling Density in points km^{-2})		
	1 (484)	2 (251)	3 (178)
Slope (Horn)	7.5 m	12.5 m	20.0 m
Slope (Zevenbergen and Thorne)	12.5 m	12.5 m	20.0 m
Plan curvature	12.5 m*	5.0 m*	5.0 m
Profile curvature	12.5 m*	7.5 m	7.5 m
Curvature	5.0 m	7.5 m	5.0 m
Wetness Index	5.0 m	5.0 m	5.0 m

Test results of the Kolmogorov-Smirnov test for tested features and three study areas. The grid cell size reported is that grid cell size where values derived from smaller grid cell sizes are not significantly different. The next larger grid cell size would result in a value that is significantly different at the 95% confidence level (* marks a 99% confidence level).

All results are listed in Table 4. Results from this test show at what resolution all relevant terrain information has been extracted from the source point data, and further refinement of the DTM resolution would not significantly change the tested terrain derivatives. Results for DEM_{100} show that first order derivatives can be based on DEMs with a 7.5 m grid cell size for steep terrains, while flat terrains can be represented with a 20 m resolution. A rule for slope becomes apparent in that the smaller the sampling density (the flatter the terrain), the coarser the slope grid can be. For Study Area 1 slight differences exist depending on the slope algorithm used.

Distributions of second order derivatives (plan and profile curvature) show a reverse trend: the higher the sampling density (the steeper the terrain) the coarser the grid cell size can be. For plan curvature, the cell sizes range from 12.5 for Study Area 1 to 5 m for Study Area 3.

For both compound terrain derivatives investigated (curvature and the wetness index), the smallest grid resolution examined (5 m) shows a significantly different distribution to the 7.5 m and larger grid cell sizes. One exception is the representation of curvature in Study Area 2, where the 5 m grid cell size is not significantly different from the 7.5 m grid, and therefore the 7.5 m grid reveals the best information. Based on these results, researchers using the province-wide Alberta elevation points should be aware that grid cell sizes reported in Table 4 contain the best information that can be extracted from the original source data. It must be kept in mind, however, that the use of the reported grid cell sizes is no guarantee for realistic spatial representation of these terrain variables, as was shown earlier.

3.7.3 Optimization of Grid Cell Size Using the Root Mean Square Measure

Another measure to qualify the optimum grid cell size is to calculate the RMS of terrain derivatives and plot them against the grid cell size. This method was applied by Hutchinson (1996) and Hutchinson and Gallant (2000). The criterion for an optimum grid cell size is found at the point in the graph where the RMS value starts to flatten. RMS slope

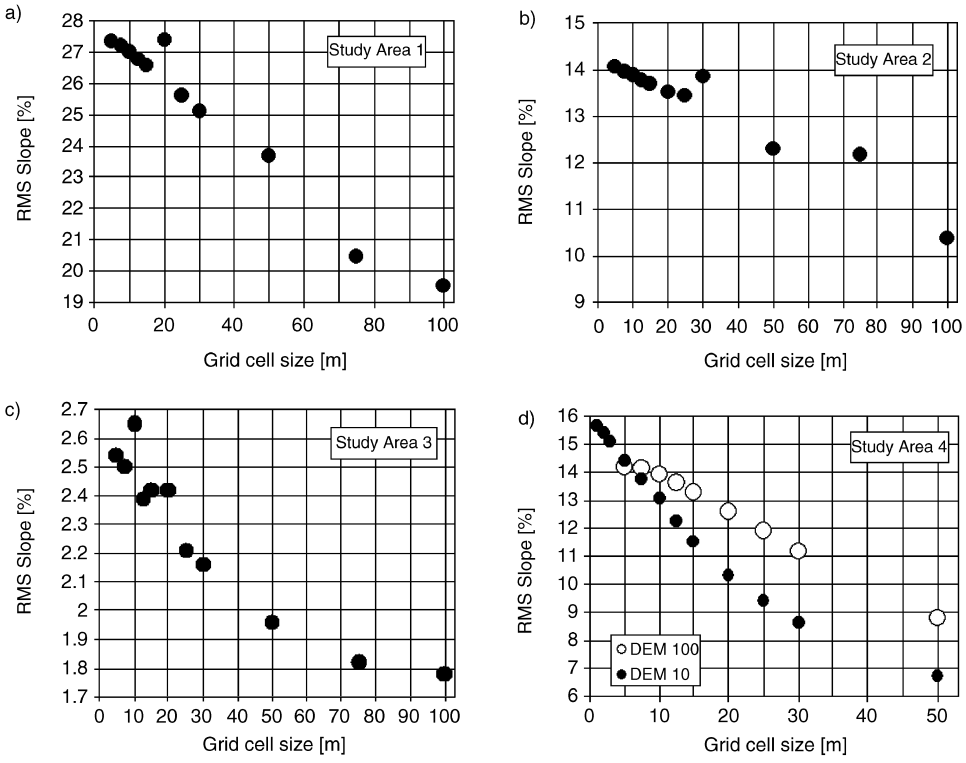

Figure 13 Root mean square slopes for four study areas and a range of grid cell sizes

values are plotted against grid cell size for all four study areas in Figure 13. For Study Area 1, a minor flattening is apparent at a grid cell size of 7.5 m, which conforms with the results of the Kolmogorov-Smirnov test shown in Table 4. However, an outlier exists at a grid cell size of 20 m, which could either be the result of the localized grid cells (where a shift in grid cell location could result in different RMS slope values), or it could be the indication that the information contained in the source point elevations has reached an optimum at 20 m. Two such outliers are present in Study Area 2 at grid cell sizes 75 and 30 m. No area of flattening of the RMS slope can be found here, so the results from the Kolmogorov-Smirnov test cannot be confirmed. No clear optimum grid cell size can be derived from Figure 13b. A different pattern is shown in Figure 13c for Study Area 3. RMS slope values for grid cell sizes below 20 m seem to be erratic, suggesting that an optimum grid cell size has been reached at a grid cell size of 20 m. This value again coincides with the test results reported in Table 4. In Figure 13d results for both DEM_{100} and DEM_{10} are plotted for Study Area 4. While a clear flattening on RMS slope values for DEM_{100} at a grid cell size of 7.5 m is evident, no clear flattening can be found for DEM_{10}, indicating that the optimum grid cell size for DEM_{10} for slope is 1 m or less. Since the density of source elevation points in Study Areas 1 and 4 are quite comparable (484 and 345 point km^{-2} respectively), it is interesting that the optimum grid cell size for slope analysis of 7.5 m can be qualified for both study areas.

The RMS for profile curvature and the wetness index were plotted for Study Area 4 to show general trends using this approach for compound derivatives. RMS values for

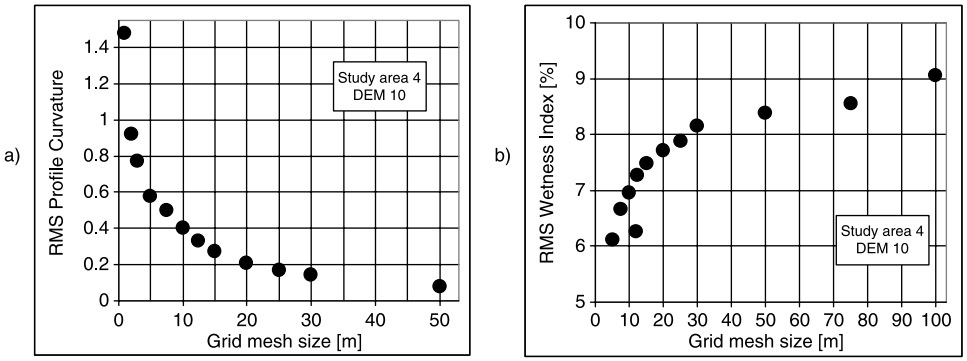

Figure 14 Root mean square profile curvature (a) and wetness index (b) for study area 4, based on DEM_{10}

profile curvature show a steady increase with grid cell size (Figure 14a), with no flattening. This is to be expected, since the profile curvature will become more severe with smaller grid cells. RMS values for the wetness index show a steady decline with decreasing grid cell size (Figure 14b). An outlier exists at a grid cell size of 12.5 m, indicating a potential optimum may have been reached at that grid cell size.

3.7.4 Testing for Correlations

The Pearson correlation coefficient is a measure of the strength of the linear relationship between two sets of data. A grid resolution of 5 m was chosen as the benchmark to compare the relationship of terrain variables derived from 10 m and 100 m regularly sampled elevation points respectively. Each 5 m grid cell containing a terrain value derived from the 10 m elevation points was correlated spatially to the relevant grid cell derived from the 100 m elevation points. Consequently, terrain values from a 5 m resolution were compared one-on-one with the benchmark grid, and terrain values with a 10 m resolution were compared to the four corresponding benchmark grid values and so forth. Only grid cell sizes ranging from 5 m to 30 m were analyzed. High correlation coefficient values, close to 1, indicate that the terrain values derived from 100 m elevation points represent the benchmark well, while low correlation coefficients indicate that a poor spatial correlation exists. Results are summarized in Table 5. There exists a strong positive correlation for elevation between the 5 m DEM based on DEM_{10} and all DEM resolutions based on DEM_{100}. There also exists a strong positive correlation for slope values, however, with grid cell sizes larger than 10 m the correlation becomes increasingly weaker. This indicates that, in agreement with Table 4, a grid cell size of 10 m or smaller is sufficient to derive slope. The striking result presented in Table 5 is that all other terrain variables based on DEM_{100} are poorly correlated with respective terrain variables based on 5 m resolution DEM_{10}. Correlations of wetness index values are nearly non-existent, even with the smallest grid resolution. The limitations of DEM_{100} for localized geomorphological, hydrological and environmental analyses are clearly evident.

3.7.5 Measuring the Quality of Terrain Variables Derived from DEM_{100}

RMS error (RMSE) is used as a measure to evaluate the quality of terrain derivatives based on DEM_{100}. It can be understood as the standard deviation of one surface against

Table 5 Pearson correlation coefficients for terrain derivatives calculated from 5 m resolution based on the DEM_{10} versus terrain derivatives calculated from a variety of grid resolutions based on the DEM_{100}

	Grid cell size					
Variable	5 m	10 m	15 m	20 m	25 m	30 m
Elevation	0.995	0.994	0.992	0.990	0.986	0.983
Slope (Horn)	0.926	0.927	0.911	0.896	0.867	0.857
Slope (Zevenbergen and Thorne)	0.928	0.928	0.915	0.899	0.879	0.857
Plan curvature	0.372	0.384	0.315	0.279	0.206	0.174
Profile curvature	0.437	0.511	0.491	0.450	0.404	0.350
Curvature	0.474	0.522	0.468	0.433	0.366	0.302
Wetness Index	0.140	0.133	0.128	0.107	0.102	0.086

All correlations are significant at the 0.01 level (2-tailed)

a benchmark surface. This analysis was only carried out for Study Area 4. RMSE is defined as:

$$\mathrm{RMSE} = \sqrt{\frac{1}{n}\sum_{i}^{n}(y_i' - y_i)^2} \tag{2}$$

where y is the cell value based on DEM_{10} with a 5 m grid resolution and y' is the respective cell value based on DEM_{100} with grid cell sizes ranging from 5 to 30 m and resampled to 5 m; and n is the number of compared points (here: 90,000).

Results for elevation, slope and the wetness index are presented in Figure 15. RMSEs for elevation values (Figure 15b) decrease from 4.3 m with a 50 m resolution to 2.0 m with the 5 m resolution. A threshold value of about 2 m is to be expected due to the large difference in sampling densities of elevation points between DEM_{10} and DEM_{100}, as is evident from Figure 7. Slope values also reach an RMSE threshold (Figure 15a). RMSEs for slopes derived using Horn's and Zevenbergen and Thorne's methods are insignificantly different, with threshold values of 4.8 and 4.9% respectively. The wetness index is generally largely overestimated (see Figure 10) with RMSEs ranging from 3.3 with a 50 m grid cell size to 2.7 with a grid cell size of 5 m.

The relative root mean square error (RRMSE) standardizes the RMSE calculated for each grid cell to the benchmark cell value (5 m grid cell size), and the derived terrain variables based on DEM_{10}. The resulting RRMSE is expressed as a percentage and represents the standard variation of the estimated terrain variable. The RRMSE is expressed as:

$$RRMSE = \sqrt{\frac{1}{n}\sum_{i}^{n}\frac{(y_i' - y_i)^2}{y_i}} \cdot 100 \tag{3}$$

with the variables as described in Equation (2).

Results are shown in Figure 16. All RRMSEs decrease with a decrease in grid cell size. RRMSEs are small for elevation values, ranging from 4.8 to 2.3%, and are large for all derivatives. RRMSEs for slope values reach a minimum of about 65% and can

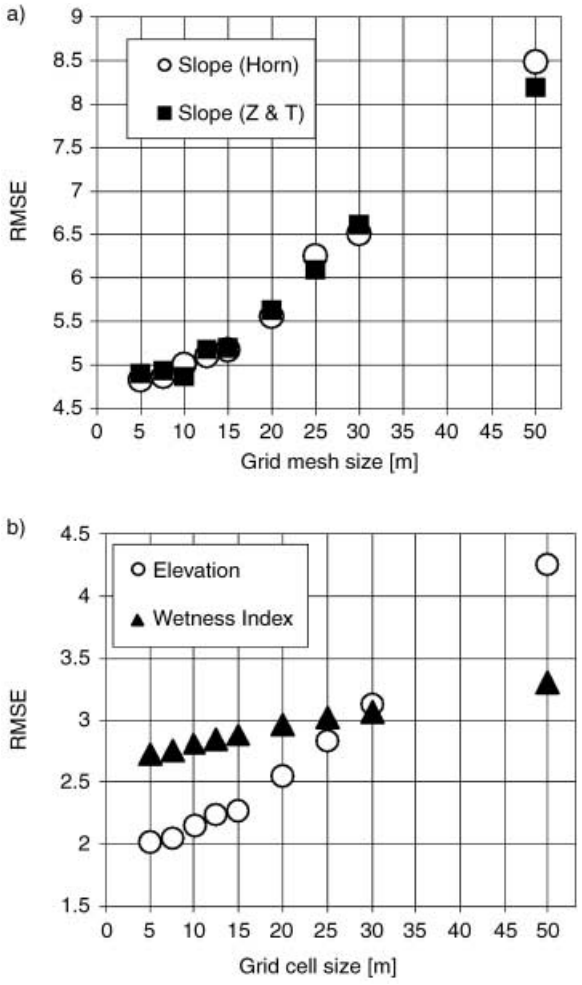

Figure 15 Root mean square errors for slope (a) and elevation and the wetness index (b) derived from a range of grid cell sizes from DEM_{10}

be larger than 100% for the coarse grid cell size of 50 m. These large values can be explained by the fact that the terrain is mainly very flat and a difference of a gentle slope such as 2% based on DEM_{100} versus a slope of 4% based on DEM_{10} will constitute a relative difference of 100%. The wetness index has RRMSEs ranging from between 50% and 42% for the grid cell sizes investigated.

The question arises, how much smaller the interpolated grid cell size must be than the source point elevations used for the interpolation? In order to answer that question, an attempt was made to use DEM_{10} and calculate the RMSE for selected terrain derivatives by using a range of grid cell sizes and comparing the various derivatives against a benchmark grid, which has been selected to have a cell size of 1 m. Results in Figure 17a show that the RMSE for elevation increases linearly with an increase in grid sell size. Results for slope in Figure 17b show that the RMSE for slope increases logarithmically with

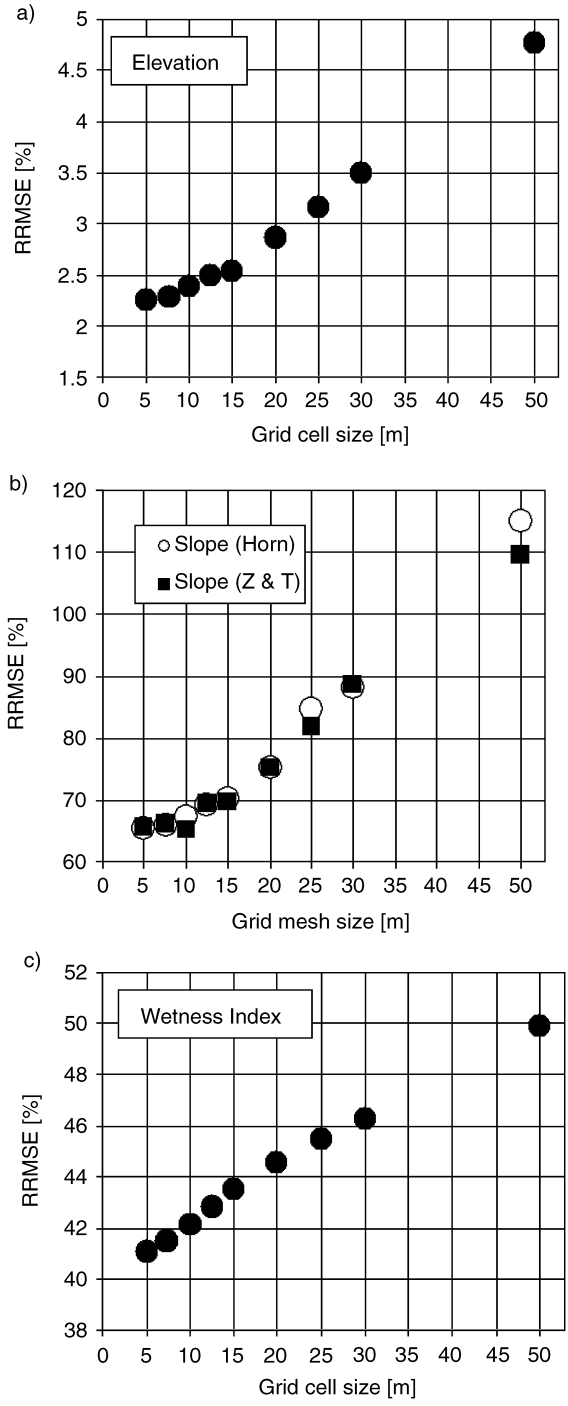

Figure 16 Relative root mean square errors for elevation (a), slope (b) and the wetness index (c) derived from a range of grid cell sizes, Study Area 4, using the respective grids with 1 m cell size as a benchmark

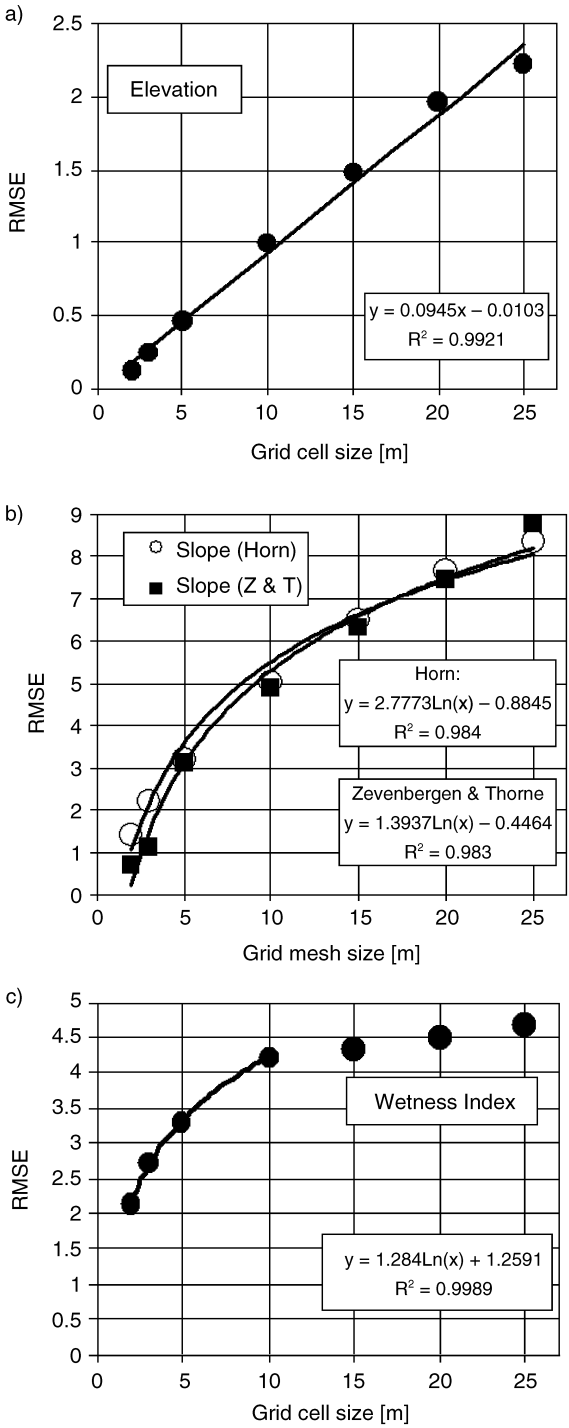

Figure 17 Root mean square errors for elevation (a), slope (b) and the wetness index (c) derived from a range of grid cell sizes from DEM_{10}, using the respective 1 m grid cell size as benchmark. The equations and the coefficient of determination describe the trend lines

an increase in grid cell resolution. The dependence of the wetness index RMSE on grid cell size shows a slightly different pattern. A threshold value of RMSE of about 4.3 seems to be reached at a grid resolution of 10 m, which is the spacing of the regularly sampled point elevations of the source of the DTM (Figure 17c). The RMSE then declines logarithmically with a decrease in grid cell size.

4 Summary and Conclusions

The results presented here have shown that DEMs generated from coarsely sampled elevation points such as those available in Alberta, Canada may have severe limitations in their use for terrain analyses. Findings reported here are valid for the world's flat to moderately sloped terrain, such as the North American plains and foothills regions.

All computed terrain variables tested (elevation, slope, aspect, plan and profile curvature, curvature and the wetness index) vary significantly with a change in grid cell size of the raster DEM. Analysis of the effect of grid cell size on slope has strengthened findings reported by other authors that slope values increase with an increase in grid cell size. These findings are in line with results reported by Zhang and Montgomery (1994) for two small catchments in Oregon. Detailed results have been shown in Figures 8a, 9, 10a, b, 13, 15a, 16b and 17b. The two most widely used methods for slope analysis are the Horn (1981) and the Zevenbergen and Thorne (1987) methods. The Horn method is implemented as the standard method in all ESRI software, while the Zevenbergen and Thorne method is available through special commands. According to Jones (1998) these two methods ranked the best. A comparison of both methods has revealed that both methods resulted in no significant differences in slope values (Figures 10a, b, 15a, 16b and 17b). Irrespective of the grid cell size used, the Horn method results, relative to the Zevenbergen and Thorne method, in slightly lower slope values. RMSEs of slope values, calculated using a 1 m grid cell size as a benchmark and comparing slope grids based on a range of grid cell sizes, show again that the Horn and Zevenbergen and Thorne methods result consistently in similar RMSEs.

Effects of the grid cell size on aspect, as the other first order terrain derivative, may also be highly significant, because aspect (or flow direction, which is calculated using a range of different algorithms) may be used, inter alia, to estimate radiation inputs and for a wealth of hydrological applications with large impacts on watershed areas and pollution sources. Instead of comparing the original aspect values, the difference in aspect angle relative to a benchmark aspect grid was calculated (Figures 10b and c). Results show that, practically independent from the grid cell size chosen, aspect angles based on DEM_{100} are out by 35-40° for 50% of the study area, out by 70–80° for 25% of the study area and may be as much out as a full 180° at certain locations. Significant effects on subsequent calculations can be expected. The consequences of these findings severely limit the uses of a DEM based on coarsely sampled elevation points for environmental and hydrological analysis, such as derivation of stream networks or the detection of pollution source areas. No meaningful differences between the two algorithms used (Horn 1981, Zevenbergen and Thorne 1987) were identified.

Similar to aspect, all other second and compound terrain derivatives based on the coarsely sampled elevation points revealed very weak to nonexistent correlations when compared to their respective benchmark grids. A DEM based on 100 m regularly sampled points can, therefore, only be used to show the general range and distribution

of terrain variables, but fails to correctly represent all tested terrain variables spatially, with the exception of slope and elevation.

An attempt was made to identify the grid cell size that maximizes the information contained in the source point elevations, using three different approaches: (a) undertaking density and distance to nearest point analysis, (b) identifying significant differences in cumulative distribution functions of terrain derivatives and (c) using the RMS slope measure.

Either density analysis or the analysis of the nearest distance to a neighbouring elevation points will reveal valuable insight into the source elevation points. Results have shown that all four study areas investigated, including a very flat area with a small river running through it, have a nearest distance of between 10 and 15 m for 10% or more of their area. Since the DEM interpolation algorithm, such as splines, kriging or ANUDEM, fit a mathematical surface to the sampled elevation points, slope, aspect or curvature values will not change linearly between those points. It follows that the grid cell size should be significantly smaller than the closest distance of sampled elevation points. It is generally accepted that most terrain does not change significantly over a short distance such as a few metres. In this study, a smallest grid cell size of 5 m for DEM_{100} and 1 m for DEM_{10} were analyzed. With the four study areas investigated, this would signify the closest 1 to 3% of elevation points, with an increase in percentile with an increase in overall terrain complexity of the study area. The smaller the sampling density (the flatter the terrain), the coarser the DEM can be for the analysis of slope, which is a first order terrain derivative. However, if second order terrain derivatives are of interest, such as plan and profile curvature, the grid cell size should increase with a decrease in the density of original point elevations. Where compound terrain derivatives, such as curvature or the wetness index, are required, generally the smallest feasible grid cell size should be selected.

The optimum grid cell size for a variety of terrain derivates was determined using the Kolmogorov-Smirnov test to identify significant differences between cumulative distribution functions. Results in Table 4 show that the optimum grid cell sizes for slope, based on DEM_{100}, vary from between 7.5 and 20 m, depending on the sampling density of the study area. The smaller the sampling density (the flatter the terrain), the coarser the grid resolution can be for slope calculations. Distributions of second order derivatives (plan and profile curvature) show a reverse trend: the higher the sampling density (the steeper the terrain) the coarser the grid cell size can be. For plan curvature, the cell sizes range from 12.5 to 5 m. For curvature and the wetness index, the smallest grid resolution examined (5 m) generally shows a significantly different distribution to the 7.5 m and larger grid cell sizes, indicating that the smallest feasible grid cell size should be used.

With one exception, results revealed using the Kolmogorov-Smirnov test were confirmed using the RMS slope measure. For slope, grid cell sizes of between 7.5 m for more complex terrain and 20 m for flat terrain were identified as the optimum grid cell sizes. This method did not reveal clear indications as to the optimum grid cell sizes for profile curvature and the wetness index.

The effect of grid cell size on terrain derivatives were further investigated by calculating the RMSE for selected terrain derivatives from DEM_{10} by using a range of grid cell sizes and comparing the various derivatives against a benchmark grid, which has been selected to have a cell size of 1 m. Results in Figure 17a show that the RMSE for elevation increases linearly with an increase in grid sell size, while RMSE for second order and compound terrain derivatives increases logarithmically with grid cell size.

Based on the reported results, researchers using point elevation data similar to the data sets available in Alberta, Canada should be aware that grid cell sizes reported in Table 4 contain the most information that can be extracted from the original source data.

With the variety of DEM sources, variety of DEM interpolation algorithms, variety of grid cell sizes used and a variety of terrain analyses algorithms available, it is very difficult to directly compare a terrain variable such as slope between study areas and across organizations. In order to allow appropriate interpretation of terrain analyses based on DEMs, both DEMs and DTMs must always be supported by detailed metadata, which should contain essential details about the DEM source, such as sampled point elevations, and any algorithms applied.

Acknowledgements

The author would like to thank Alberta Agriculture, Food and Rural Development for the initial provision of the 100 m elevation points, as well as the City of Lethbridge for making the 10 m elevation points available for Study Area 4. This research was funded by the University of Lethbridge Research Fund. My research assistants – Amber Brown, Guy Duke and Bradley Higgins – are thanked for undertaking parts of the analyses.

References

Band L E 1993 Extraction of channel networks and topographic parameters from digital elevation data. In Beven K and Kirkby M J (eds) *Channel Network Hydrology*. Chichester, John Wiley and Sons: 13–42

Beven K J and Kirkby M J 1979 A physically based, variable contributing area model of basin hydrology. *Hydrological Sciences Bulletin* 24: 43–69

Blaszcynski J S 1997 Landform characterisation with geographic information systems. *Photogrammetric Engineering and Remote Sensing* 63: 183–91

Blöschl G and Grayson R 2001 Spatial observation and interpolation. In Grayson R and Blöschl G (eds) *Spatial Patterns in Catchment Hydrology*. Cambridge, Cambridge University Press: 17–50

Burrough P E and McDonnell R A 1998 *Principles of Geographical Information Systems*. New York, Oxford University Press

Elsheikh S and Guercio R 1997 GIS topographical analysis applied to unit hydrograph models: Sensitivity to DEM resolution and threshold area. In Baumgartner M F, Schultz G A, and Johnson I (eds) *Remote Sensing and Geographic Information Systems for Design and Operation of Water Resources Systems*. Wallingford, International Association of Hydrological Sciences Publication No 242: 245–53

ESRI 2000 *ArcGIS 8.0*. Redlands, CA, Environmental Systems Research Institute

Evans I S 1980 An integrated system of terrain analysis and slope mapping. *Zeitschrift für Geomorphology* Suppl Bd 36: 274–95

Florinsky I V 1998 Accuracy of local topographic variables derived from digital elevation models. *International Journal of Geographical Information Science* 12: 47–61

Garbrecht J and Martz L W 2000 Digital elevation model issues in water resources modeling. In Maidment D R and Djokic D (eds) *Hydrologic and Hydraulic Modeling Support with Geographical Information Systems*. Redlands, CA, ESRI Press: 1–28

Gallant J C and Wilson J P 1996 TAPES-G: A grid-based terrain analysis program for the environmental sciences. *Computers and Geosciences* 22: 713–22

Helios Environmental Modeling Institute (HEMI) 1999 Hemiview. WWW document, http://www.hemisoft.com/topoview/manual/helpcontents1.htm

Hetrick W A, Rich P M, Barnes F J, and Weiss S B 1993a GIS-based solar radiation flux models. *American Society for Photogrammetry and Remote Sensing Technical Papers* (Volume 3, GIS Photogrammetry and Modeling): 132–43

Hetrick W A, Rich P M, and Weiss S B 1993b Modeling insolation on complex surfaces. In *Proceedings of the Thirteenth Annual International ESRI User Conference*, Palm Springs, California: 447–58

Horn B K P 1981 Hill shading and the reflectance map. *Proceedings of the IEEE* 69: 14–47

Hofierka J, Paraijka J, Mitasova H, and Mitas L 2002 Multivariate interpolation of precipitation using regularized spline with tension. *Transactions in GIS* 6: 135–50

Hutchinson M F 1988 Calculation of hydrologically sound digital elevation models. In *Proceedings of the Third International Symposium on Spatial Data Handling*, Sydney, Australia

Hutchinson M F 1989 A new procedure for gridding elevation and stream line data with automatic removal of spurious pits. *Journal of Hydrology* 106: 211–32

Hutchinson M F and Dowling T I 1991 A continental hydrological assessment of a new grid based digital elevation model of Australia. *Hydrological Processes* 5: 45–58

Hutchinson M F 1996 A locally adaptive approach to the interpolation of digital elevation models. In *Proceedings of the Third International Conference/Workshop on Integrating GIS and Environmental Modeling*. Santa Barbara, CA, University of California, National Center for Geographic Information and Analysis: CD-ROM

Hutchinson M F and Gallant J C 2000 Digital elevation models and representation of terrain shape. In Wilson J P and Gallant J C (eds) *Terrain Analysis: Principles and Applications*. John Wiley & Sons: 29–50

Jenson S K and Domingue J O 1988 Extracting topographic structure from digital elevation data for geographical information system analysis. *Photogrammetric Engineering and Remote Sensing* 54: 1593–1600

Jones K H 1998 A comparison of algorithms used to compute hill slope as a property of the DEM. *Computers and Geosciences* 24: 315–23

Kern T J and Stednick J D 1993 Identification of heavy metal concentrations in surface waters through coupling of GIS and hydrochemical models. In Kovar K and Nachtnebel H P (eds) *Application of Geographic Information Systems in Hydrology and Water Resources Management*. Wallingford, International Association of Hydrological Sciences Publication No 211: 559–67

Kienzle S W 1994 The application of a GIS-Grid system for hydrological and geomorphological analysis. In *Proceedings of the Fourth Symposium on Terrain Evaluation and Data Storage*, 3–5 August, Midrand, South Africa

Kienzle S W, Lorentz S A, and Schulze R E 1997 *Hydrology and Water Quality of the Mgeni Catchment*. Pretoria, Water Research Commission Report No TT87/97

Klaghofer E, Birnbaum W, and Summer W 1993 Linking sediment and nutrient export models with a geographic information system. In Kovar K and Nachtnebel H P (eds) *Application of Geographic Information Systems in Hydrology and Water Resources Management*. Wallingford, International Association of Hydrological Sciences Publication No 211: 501–6

Macmillan R A, Pettapiece W W, Nolan S C, and Goddard T W 2000 A generic procedure for automatically segmenting landforms into landform elements using DEMs, heuristic rules and fuzzy logic. *Fuzzy Sets and Systems* 112: 81–109

Martz L W and Garbrecht J 1992 Numerical definition of drainage network and subcatchment areas from digital elevation models. *Computers and Geosciences* 18: 747–61

Mitasova H, Hofierka J, Zlocha M, and Iverson L R 1996 Modeling topographic potential for erosion and deposition using GIS. *International Journal of Geographical Information Science* 10: 629–41

Moore I D, Grayson R B, and Ladson A R 1991 Digital terrain modelling: A review of hydrological, geomorphological and biological applications. *Hydrological Processes* 5: 3–30

Moore I D, Turner A K, Wilson J P, Jenson S K, and Band LE 1993 GIS and land surface–subsurface process modeling. In Goodchild M F, Parks B O, and Steyaert L T (eds) *Environmental Modeling with GIS*. New York, Oxford University Press: 197–230

Quinn P F and Beven K J 1993 Spatial and temporal prediction of soil moisture dynamics, runoff, variable source areas and evapotranspiration for Plynlimon, mid-Wales. *Hydrological Processes* 7: 425–48

Saulnier G, Obled C, and Beven K 1997 Analytical compensation between DTM grid resolution and effective values of saturated hydraulic conductivity within the TOPMODEL framework. *Hydrological Processes* 11: 1331–46

Tarboton D G, Bras R L and Rodriguez-Iturbe I 1991 On the extraction of channel networks from digital elevation data. *Hydrological Processes* 5: 81–100

Zevenbergen L W and Thorne C R 1987 Quantitative analysis of land surface topography. *Earth Surface Processes and Landforms* 12: 47–56

Zhang W and Montgomery D R 1994 Digital elevation model grid size, landscape representation, and hydrologic simulations. *Water Resources Research* 30: 1019–28